

## Multi-focus Image Fusion with Cartoon-Texture Image Decomposition

Yongxin Zhang<sup>1</sup>, Hongan Li<sup>2</sup> and Zhihua Zhao<sup>3</sup>

<sup>1</sup>*School of Information Technology, Luoyang Normal University, Luoyang, 471022, China*

<sup>2</sup>*School of Computer Science and Technology, Xi'an University of Science and Technology, 710054, China*

<sup>3</sup>*Department of Information Engineering, ShanXi Conservancy Technical College, Yuncheng, 044004, China  
tabo126@126.com*

### Abstract

*Multi-focus image fusion can fuse multiple source images with different focus settings into a single image that appears sharper. How to effectively and completely represent the source images is the key to multi-focus image fusion. A multi-component fusion method is proposed for multi-focus image fusion. The registered source images are decomposed into cartoon and texture components by cartoon-texture image decomposition. The salient features are selected from the cartoon and texture components respectively to form a composite feature space. The local features that represent the salient information of the source images are integrated to construct the fused image. According to the visual perception and objective evaluations on the fused images, the proposed method works better in extracting the focused regions and improving the fusion quality, compared with the other existing single-component fusion methods.*

**Keywords:** *image fusion; cartoon-texture image decomposition; cartoon-texture; Split Bregman iteration; sliding window*

### 1. Introduction

Image fusion aims to produce a single sharper image by combining a set of images captured from the same scene with different focus points [1]. In general, the image fusion methods can be categorized into two groups: spatial domain fusion and transform domain fusion [2]. This paper particularly focuses on the spatial domain methods.

The spatial domain methods are easy to implement and have low computational complexity. The spatial domain fusion methods can be divided into pixel based methods and region based methods. The pixel based methods is to take the average of the source images pixel and pixel. The region based methods partition the source images into blocks or regions by using their region homogeneity, and detect the focused blocks or regions by using their local spatial features [3], such as energy of image gradient (EOG) [4] and spatial frequency (SF) [5]. Then, the focused blocks or regions are integrated into the counterparts of the fused image. However, if the size of the blocks is too small, the blocks selection is so sensitive to noise that incorrect selection from the corresponding source images. Or else, if the size of the blocks is too large, the in-focus and out-of-focus pixels are partitioned in the same blocks, which are selected to build the final fused image. Accordingly, the blocking artifacts are produced and may compromise the quality of the final fused image. Researchers have developed many improved schemes to eliminating the blocking artifacts. Goshtasby *et al.*, [6] have detected the focused blocks by computing the weight sum of the blocks. The iterative procedure is time-consuming. Fedorov *et al.*, [7] have selected the best focus by titling source images with overlapping

neighborhoods and improved the visual quality of the fused image. But this method is afflicted by temporal and geometric distortions between images. Aslantas *et al.*, [8] have selected the optimal block-size by using differential evolution algorithm and enhanced the self-adaptation of the fusion method. But this method requires longer computational time. Jiang *et al.*, [9] have fused source images by using morphological component analysis. But the algorithm is complicated and time-consuming. Zhang *et al.*, [10] have determined the optimal block-size by using quad tree structure and effectively solved the problem of determining of block-size. These schemes all achieve better performance than the traditional methods and significantly inhibit the blocking artifacts. But they cannot eliminate the blocking artifacts completely.

Different from the fusion methods mentioned above, in order to effectively and completely represent the source images, a novel fusion method based on cartoon-texture image decomposition is proposed. Cartoon-Texture image decomposition is an important way of image processing, which has been widely used in image analysis and vision applications, such as enhancement, inpainting, segmentation, texture and shape analysis [11]. Cartoon-Texture image decomposition separates a given image into cartoon and texture components. The cartoon component holds the geometric structures, isophotes and smooth-piece of the source images, while the texture component contains textures, oscillating patterns, fine details and noise [9]. The cartoon and texture components represent the most meaningful information of the source images, which are important for image fusion. Cartoon-Texture image decomposition has been proven to be an effective way to extract the structure information and texture information from the image [12]. The objective of this paper is to investigate the potential application of cartoon-texture image decomposition in the multi-focus image fusion. The main contribution of this paper is that a multi-component fusion framework is established. The pixels belonging to the focused regions are detected by the discriminative features that computed from the cartoon and texture components of the source images. The proposed method works well in inhibiting the blocking artifacts and representing the source images.

The rest of the paper is organized as follows. In Section 2, the basic idea of cartoon-texture image decomposition will be briefly described, followed by the proposed method in Section 3. In Section 4, extensive simulations are performed to evaluate the performance of the proposed method. In addition, several experimental results are presented and discussed. Finally, concluding remarks are drawn in Section 5.

## 2. Cartoon-Texture Image Decomposition

Nowadays, an observed image  $f$  represents a real scene in many problems of image analysis [13]. The image  $f$  may contain texture or noise. In order to extract the most meaningful information from  $f$ , most models try to find another image  $u$ , “close” to  $f$ , such that  $u$  is a cartoon or simplification of  $f$ . These models assume that there is a relation between  $f$  and  $u$  as follows:

$$f = u + v \quad (1)$$

where  $v$  is noise or texture.

Mumford D. and Shah J. [14] have established a model to decompose the black and white static image by using bounded variation function, which is called Mumford-Shah energy functional:

$$E_{MS}(u, C) = \iint_{R \setminus C} (\|\nabla u\|^2 + \lambda(u - u_0)) dx dy + \mu Len(C) \quad (2)$$

where  $C$  is the segmenting contour,  $\lambda > 0$  and  $\mu > 0$  are the weight coefficients.  $u_0$  is the feature of the original image.  $u$  is the optimal piecewise approximation of  $u_0$ .

Rudin *et al.*, [15] have simplified the Mumford-Shah model and proposed total variation minimization energy functional model of Rudin-Osher-Fatemi (ROF) as:

$$E_{ROF}(u) = \iint_R (\|\nabla u\| dx dy + \lambda \iint_R (u - u_0)^2 dx dy) \quad (3)$$

where  $\lambda > 0$  is the weight coefficient.

The ROF model is very efficient for de-noising images while keeping sharp edges. In fact, Both Mumford-Shah model and ROF model can minimize the energy function that they have constructed, and obtain the correct decomposition of the source image. But Meyer Y. [16] has proved that the ROF model will remove the texture when  $\lambda$  is small enough. In addition, he has introduced the use of a space of functions, which is the dual of the  $BV$  space in some sense.

Vese and Osher [17] have combined the total variation minimization in image restoration of ROF model with the ideas introduced by Meyer to model texture or noise. The model is described as:

$$E_{Vo}(u, \vec{g}) = \iint_R (\|\nabla u\| dx dy + \lambda \iint_R |u_0 - (u + \text{div}(\vec{g}))|^2 dx dy + \mu \|\vec{g}\|_{L^p}) \quad (4)$$

They have developed a partial differential equation (PDE) based on iterative numerical algorithm to approximate Meyer's weaker norm  $\|\cdot\|_G$  by using  $L^p$ . But this model is time consuming. To improve the computation efficiency, many models and methods have been proposed. Osher S. *et al.*, [18] have developed Osher-Sole-Vese (OSV) model based on total variation (TV) and norm  $H^{-1}$ . Chana *et al.*, [19] have proposed  $CEP - H^{-1}$  model based on OSV. But these methods are still complicated. Goldstein T. and Osher S. [20] have proposed Split Bregman algorithm by combining the split method [21] with Bregman iteration [22]. This algorithm is easy to implement and has low computational complexity. This paper performs the cartoon-texture image decomposition on the source images based on ROF model by using Split Bregman algorithm.

Figure 1 shows the cartoon-texture decomposition results of the source images 'Clock'. It is obvious that the salient features of the cartoon and texture components of the source image are corresponding to the local feature of the clock in focus. Thus, the cartoon and texture components can be used to build a robust fusion scheme to discriminate the focused regions from defocused regions. In this paper, the salient features of the cartoon and texture components are used to detect the pixels belonging to the focused regions.

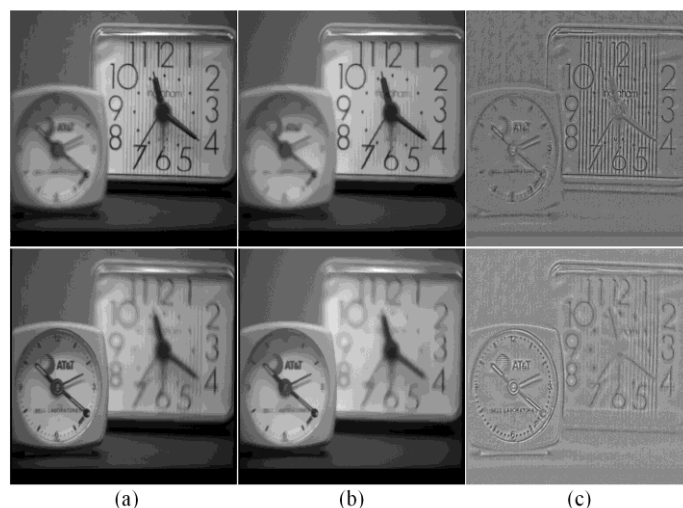


**Figure 1. Decomposition of Multi-Focus Images 'Clock' Using Cartoon-Texture Image Decomposition. (a) Source Images, (b) Cartoon Components, (c) Texture Components**

### 3. Proposed Method

#### 3.1. Fusion Algorithm

In this section, a novel method based on image decomposition is proposed. The source images must be initially decomposed into cartoon and texture components, respectively. Then, both components are integrated according to certain fusion rules, respectively. The proposed fusion framework is depicted in Figure 2 and the detailed design is described as follows. For simplicity, this paper assumes that there are only two source images, namely  $I_A$  and  $I_B$ , here. The rationale behind the proposed scheme applies to the fusion of more than two multi-focus images. The source images are assumed to be pre-registered and the image registration is not included in the framework. The fusion algorithm consists of the following 3 steps:

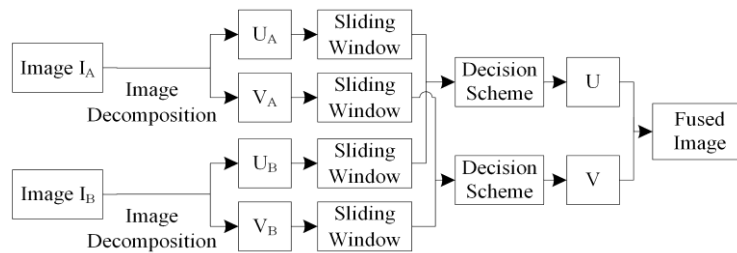


**Figure 2. Block Diagram of Proposed Multi-focus Images Fusion Framework**

Step 1: Perform the cartoon-texture image decomposition on the source images  $I_A, I_B$  to obtain cartoon and texture components, respectively. For the source image  $I_A$ , let  $U_A, V_A$  denote the cartoon and texture components, respectively. For the source image  $I_B$ ,  $U_B, V_B$  have the roles similar to  $U_A$  and  $V_A$ .

Step 2: According to the fusion rules,  $U_A$  and  $U_B$  are integrated to obtain  $U$  which denotes the cartoon component of the fused image. Similarly,  $V_A$  and  $V_B$  are combined to form  $V$  which denotes the texture component of the fused image.

Step 3:  $U$  and  $V$  are superposed to form the fused image  $F$ .

#### 3.2. Fusion Rule

There are two key issues [9] involved with the fusion rules. The first is how to measure the activity level of the source images, which recognizes the sharpness of the source images. Figure 3 shows the relationship between multi-component of the source images ‘Clock’ and their 3D shapes. It is obvious that the salient protruding portions of the 3D shapes of the multi-component are corresponding to the salient regions of the cartoon and texture components, and the salient regions of the cartoon and texture components are corresponding to the focused regions of the source images. Thus, we use the EOG of the pixels within a  $M \times N$  ( $M = 2s + 1, N = 2t + 1$ ) window of the cartoon and texture components to measure the activity level, respectively.  $s$  and  $t$  are all positive integers. The EOG is calculated as:

$$\begin{cases} EOG(i, j) = \sum_{m=-(M-1)/2}^{(M-1)/2} \sum_{n=-(N-1)/2}^{(N-1)/2} (I_{i+m}^2 + I_{j+n}^2) \\ I_{i+m} = I(i+m+1, j) - I(i+m, j) \\ I_{j+n} = I(i, j+n+1) - I(i, j+n) \end{cases} \quad (5)$$

where  $I(i, j)$  indicates the value of the pixel location  $(i, j)$  in the cartoon or texture components. The size of the window is set as  $5 \times 5$ .

The other is how to integrate the focused pixels or regions from the cartoon and texture components into the counterparts of the fused image. In order to eliminate the blocking artifacts, a sliding window technique is applied to the cartoon and texture components, respectively. Let  $EOG_{(i,j)}^{U_A}$  and  $EOG_{(i,j)}^{U_B}$  denote the EOG of all the pixels within the sliding windows which cover the neighborhood region of the pixel location  $(i, j)$  in  $U_A$  and  $U_B$ , respectively. The  $EOG_{(i,j)}^{V_A}$  and  $EOG_{(i,j)}^{V_B}$  have the roles similar to  $EOG_{(i,j)}^{U_A}$  and  $EOG_{(i,j)}^{U_B}$  for the pixel location  $(i, j)$  in  $V_A$  and  $V_B$ . The EOG of the neighborhood region of the pixel location  $(i, j)$  in  $U_A, U_B, V_A$  and  $V_B$  are respectively compared to determine which pixel is likely to belong to the focused regions. Two decision matrices  $H^U$  and  $H^V$  are constructed for recording the comparison results according to the selection rules as follows:

$$H^U(i, j) = \begin{cases} 1, & EOG_{(i,j)}^{U_A} \geq EOG_{(i,j)}^{U_B} \\ 0, & otherwise \end{cases} \quad (6)$$

$$H^V(i, j) = \begin{cases} 1, & EOG_{(i,j)}^{V_A} \geq EOG_{(i,j)}^{V_B} \\ 0, & otherwise \end{cases} \quad (7)$$

where “1” in  $H^U$  indicates the pixel location  $(i, j)$  in image  $U_A$  is in focus while “0” in  $H^U$  indicates the pixel location  $(i, j)$  in image  $U_B$  is in focus. Likewise, the “1” in  $H^V$  indicates the pixel location  $(i, j)$  in image  $V_A$  is in focus while “0” in  $H^V$  indicates the pixel location  $(i, j)$  in image  $V_B$  is in focus.

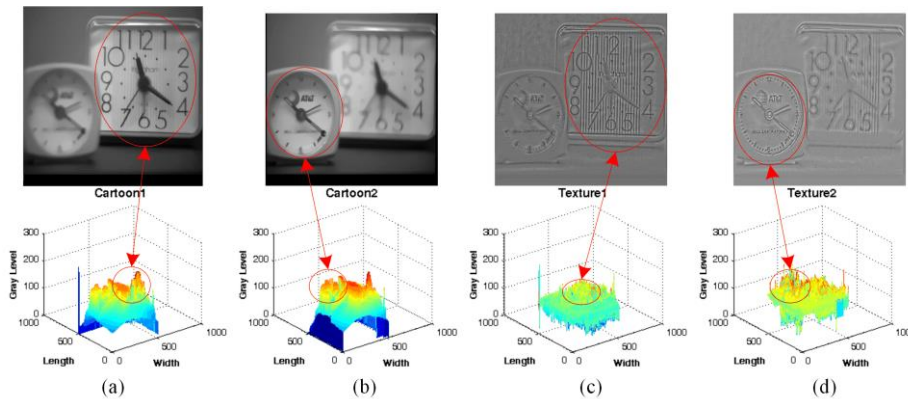


**Figure 3. The Relationship between Multi-Component of the Source Images ‘Clock’ and their 3D Shapes: (a) Cartoon Component of the Far Focused Image, (b) Cartoon Component of the Near Focused Image, (c) Texture Component of the Far Focused Image, (d) Texture Component of the Near Focused Image**

However, judging by EOG alone is not sufficient to distinguish all the focused pixels. There are thin protrusions, narrow breaks, thin gulfs, small holes, etc. in  $H^U$  and  $H^V$ . To overcome these disadvantages, morphological operations [23] are performed on  $H^U$  and  $H^V$ , respectively. Opening, denoted as  $H^U \circ Z$  and  $H^V \circ Z$ , is simply erosion of  $H^U$  and  $H^V$  by the structure element  $Z$ , followed by dilation of the result by  $Z$ . This process can remove thin gulfs and thin protrusions. Closing, denoted as  $H^U \bullet Z$  and  $H^V \bullet Z$ , is dilation, followed by erosion. It can join narrow breaks and thin gulfs. To correctly judge the small holes, a threshold is set to remove the holes smaller than the threshold. Thus, the final fused cartoon and texture components are constructed according to the rules as follows:

$$U(i, j) = \begin{cases} U_A(i, j), & H^U(i, j) = 1 \\ U_B(i, j), & H^U(i, j) = 0 \end{cases} \quad (8)$$

$$V(i, j) = \begin{cases} V_A(i, j), & H^V(i, j) = 1 \\ V_B(i, j), & H^V(i, j) = 0 \end{cases} \quad (9)$$

In this paper, the structure element  $Z$  of the proposed method is a  $5 \times 5$  matrix with logical 1's and the threshold is set to 1000.

#### 4. Experimental Results

In order to evaluate the performance of the proposed method, several experiments are performed on two pairs of multi-focus source images [24] as shown in Figure 4. The two pairs are all gray scale images with size of  $640 \times 480$  pixels. In general, image registration should be performed before image fusion. In this paper, all the source images are assumed to have been registered. Experiments are conducted with Matlab R2011b in Windows environment on a computer with Intel Xeon X5570 and 48G memory. For comparison, besides the proposed method, some existing multi-focus image fusion methods are also implemented on the same set of source images. These methods include laplacian pyramid (LAP), discrete wavelet transform (DWT), nonsubsampled contourlet transform (NSCT), principal component analysis (PCA) and SF [3]. The image fusion toolbox [25] is used as a reference for LAP, DWT, PCA and SF. Specifically, the Daubechies wavelet function 'bi97' is used in the DWT. The decomposition level of DWT and LAP is 4. The NSCT toolbox [26] is used as the reference for NSCT. The pyramid filter '9-7' and the orientation filter '7-9' with {4, 4, 3} levels of decomposition are set for the fusion method based on NSCT. The Split Bregman toolbox [27] is used as the reference for the proposed method. In order to quantitatively compare the performance of the proposed method with that of the other methods mentioned above, three metrics are used to evaluate the fusion performance: (i) Structural similarity (SSIM), which reveals the degree of structural similarity between two images in luminance, contrast and structure [28, 29]. (ii) Mutual information (MI) [30], which measures the degree of dependence of the source image and the fused image. (iii)  $\varrho^{A/B/F}$  [31], which reflects the amount of edge information transferred from the source images to the fused image. In these methods, a larger value signifies a better fusion result.

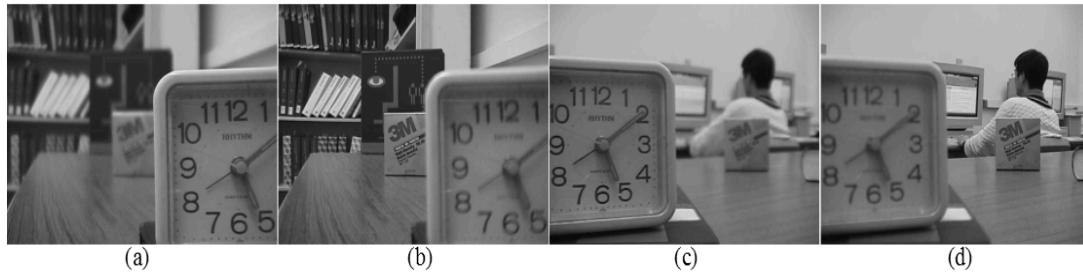


**Figure 4. Multi-focus Source Images. (a) Near Focused Image 'Disk', (b) Far Focused Image 'Disk', (c) Near Focused Image 'Lab', (d) Far Focused Image 'Lab'**

#### 4.1. Qualitative Analysis

For qualitative comparison, the fused images 'Disk' and 'Lab' obtained by different methods are shown in Figures 5 (a-f) and Figures 6 (a-f). The difference images between the far focused source image 'Lab' and corresponding fused images obtained by different methods are shown in Figures 7 (a-f).

Inspecting the book and the clock in Figure 5, there are some blurry regions in the white books of the fused images of LAP, DWT, NSCT, PCA and SF. Moreover, the obvious blocking artifacts appear in the upper edge of the clock in the fused image of SF. The contrast of the fused image of PCA is worse than that of the other methods and the contrast of the fused image of proposed method is better than the other methods. Inspecting the student and the clock in Figure 6, the student's head in the fused images of LAP, DWT and NSCT shows obvious mis-registration, respectively. In Figure 7, distortions are obviously observed in the difference images of DWT and NSCT. Mis-registration is also shown in the difference image of PCA. In addition, there are some obvious blocking artifacts in the difference image of SF. Thus, the fused image of proposed method achieves superior visual performance by containing all the focused contents from the source images without introducing artifacts.

#### 4.2. Quantitative Analysis

For quantitative comparison, the quantitative results on grayscale multi-focus images in three quality measures and the running times are also shown in Table 1. The proposed method gains highest MI and  $Q^{AB/F}$  values, except for the "Disk" images when the PCA-based method is rated highest using the SSIM measure. One can see that the running time of the proposed method is larger than that of the other methods except for NSCT. Due to the sliding window technique is applied for the detection of focused regions, the computation of EOG of all pixels of each sliding window in the proposed method requires longer computational time.

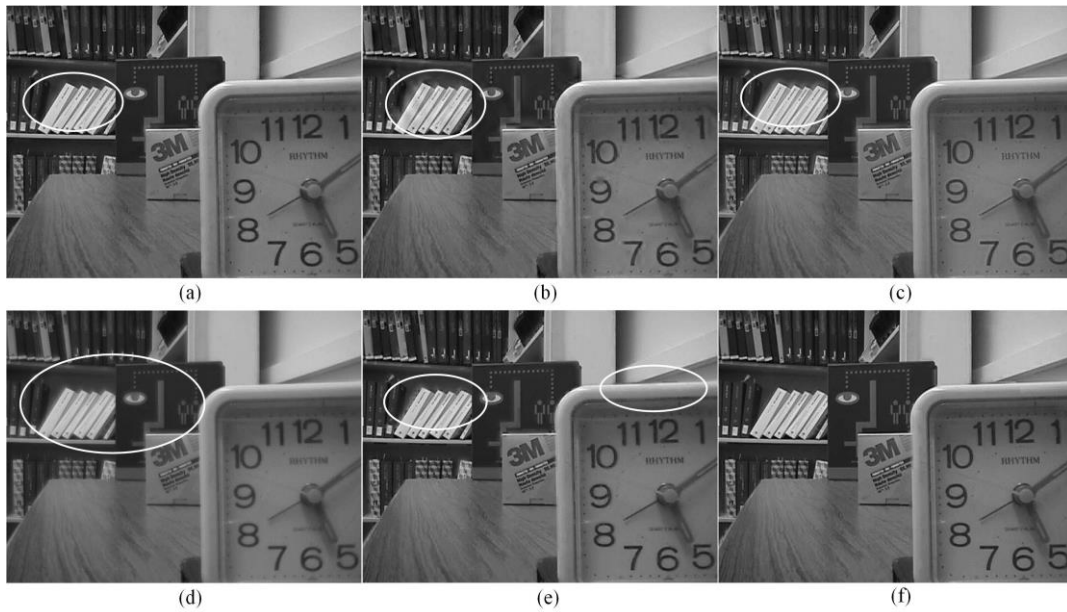


**Figure 5. Fused Images 'Disk' Obtained by LAP (a), DWT (b), NSCT (c), PCA (d), SF (e), and the Proposed Method (f)**

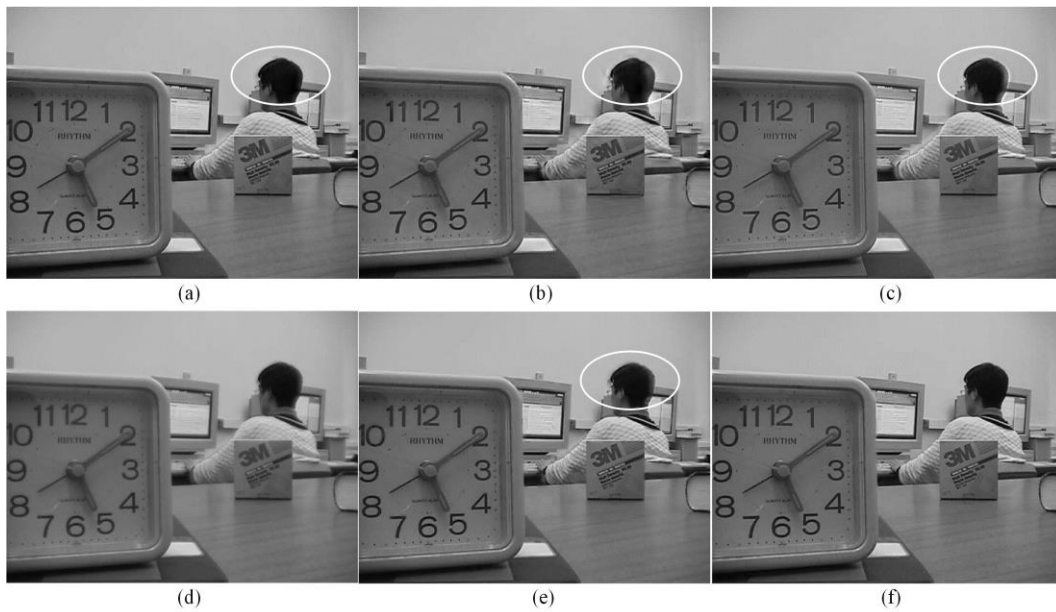


**Figure 6. Fused Images 'Lab' Obtained by LAP (a), DWT (b), NSCT (c), PCA (d), SF (e), and the Proposed Method (f)**

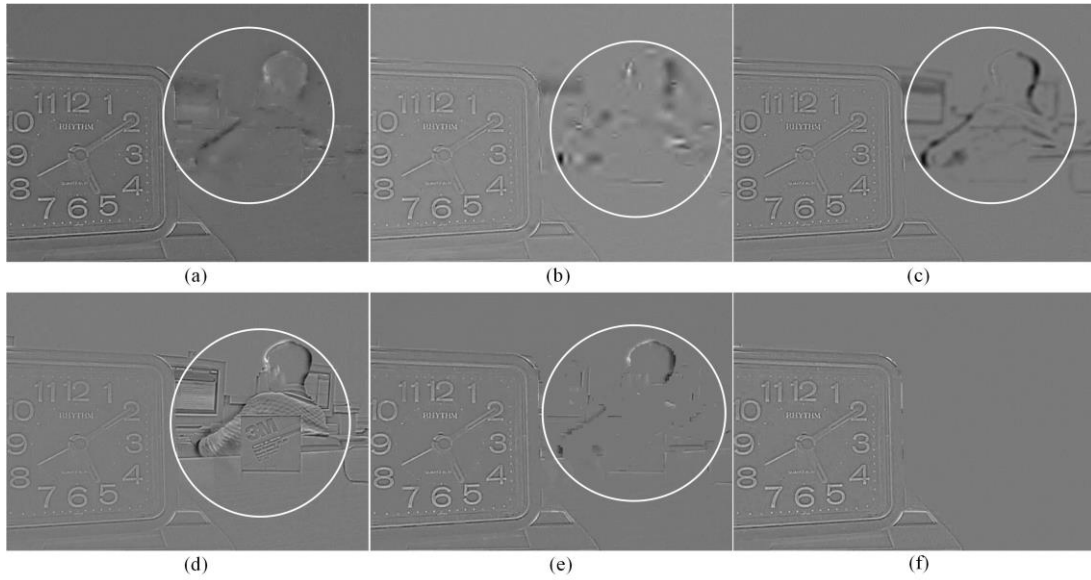


**Figure 7. Difference Images between Source Image ‘Lab’ Far Focused and Corresponding Fused Images Obtained by LAP (a), DWT (b), NSCT (c), PCA (d), SF (e), and the Proposed Method (f)**

**Table 1. Performance of Different Fusion Methods**

Method	Disk				Lab			
	SSIM	MI	$Q^{A/B/F}$	Run-time(s)	SSIM	MI	$Q^{A/B/F}$	Run-time(s)
LAP	0.86	6.14	0.69	0.91	0.91	7.10	0.71	0.91
DWT	0.84	5.36	0.64	0.64	0.90	6.47	0.69	0.59
NSCT	0.86	5.88	0.67	463.20	0.91	6.95	0.71	468.51
PCA	<b>0.91</b>	6.02	0.53	0.11	<b>0.94</b>	7.12	0.59	0.08
SF	0.87	7.00	0.68	1.01	0.91	7.94	0.72	1.03
Proposed	0.90	<b>7.25</b>	<b>0.72</b>	21.08	<b>0.94</b>	<b>8.20</b>	<b>0.75</b>	17.09

## 5. Conclusion and Future Work

This paper proposes a novel multi-focus image fusion method based on cartoon-texture image decomposition. The cartoon-texture image decomposition technique is used to decompose the registered source images into cartoon and texture components. The salient features computed from the cartoon and texture components are able to represent the salient information from the source images. The qualitative and quantitative evaluation have demonstrated that the proposed method achieves superior fusion results compared to the other existing fusion methods and significantly improves the quality of the fused image. In the future, we will consider optimizing the proposed method to reduce the time-consuming.

## Acknowledgements

The work is supported by the National Key Technology Science and Technique Support Program (No. 2013BAH49F03), the National Nature Science Foundation of China (No. 61379010), the Key Technologies R&D Program of Henan Province (No. 142102210637), the Natural Science Basic Research Plan in Shaanxi Province of China (No. 2012JQ1012).

## References

- [1] H. Hariharan, "Extending Depth of Field via Multi-focus Fusion", PhD Thesis, the University of Tennessee, Knoxville, (2011).
- [2] S. Li, X. Kang, J.Hu, B. Yang, "Image matting for fusion of multi-focus images in dynamic scenes", *Information Fusion*, vol.14, (2013).
- [3] W. Huang, Z. Jing, "Evaluation of focus measures in multi-focus image fusion", *Pattern Recognition Letters*, vol. 28, no. 9, (2007).
- [4] A.M. Eskicioglu, P.S. Fisher, "Image quality measures and their performance", *IEEE Trans. Communication*, vol. 43, no. 12, (1995).
- [5] S. Li, J. Kwok, Y. Wang, "Multifocus image fusion using the spatial frequency", *Information fusion*, vol. 28, no. 9, (2001).
- [6] A. Goshtasby, "Fusion of multifocus images to maximize image information", *Proceedings of SPIE Defense and Security Symposium*, (2006), April 17-21, Orlando, Florida.
- [7] D. Fedorov, B. Sumengen, B.S. Manjunath, "Multi-focus imaging using local focus estimation and mosaicking", *Image Processing, IEEE International Conference on Image Processing*, (2006), October 8-11, Atlanta, Georgia.
- [8] V. Aslantas, R. Kurban, "Fusion of multi-focus images using differential evolution algorithm", *Expert System with Application*, vol. 37, no. 12, (2010).
- [9] Y. Jiang, M. Wang, "Image fusion with morphological component analysis", *Information Fusion*, vol. 18, (2014).
- [10] Y. Zhang, L. Chen, Z. Zhao, J. Jia "Multi-focus image fusion using sparse feature", *International Journal of Signal Processing, Image Processing and Pattern Recognition*, vol. 7, no. 2, (2014).
- [11] Y. Li, X. Feng, "Image decomposition via learning the morphological diversity", *Pattern Recognition Letter*. vol.33, no.2, (2012).
- [12] W. Casaca, A. Paiva, E. Gomez-Nieto, P. Joia, L. Gustavo, "Spectral Image Segmentation Using Image Decomposition and Inner Product-Based Metric", *Journal of Mathematical Imaging and Vision*, vol.45,no.3, (2013).
- [13] Z. Guo, J. Yin, Q. Liu, "On a reaction-diffusion system applied to image decomposition and restoration", *Mathematical and computer modeling*, vol.53, no.5-6, (2011).
- [14] D. Mumford., J. Shah, "Optimal Approximations by Piecewise Smooth Functions and Associated Variational Problems", *Communications on Pure and Applied Mathematics*. vol.42, no.5, (1989).
- [15] L. Rudin, S. Osher, E. Fatemi, "Nonlinear Total Variation based Noise Removal Algorithms", *Phys. D: Nonlinear Phenom*, vol.60, no.1-4, (1992).
- [16] Y. Meyer, "Oscillating Patterns in Image Processing and Nonlinear Evolution Equations", *University Lecture Series*. AMS, (2001).
- [17] L. Vese, S. Osher, "Modeling textures with total variation minimization and oscillating patterns in image processing", *SIAM J. Sci. Computer*, Vol.19, no.1-3, (2003).
- [18] S. Osher, A. Sole, L. Vese, "Image Decomposition and Restoration Using Total Variation Minimization and the H-1 Norm", *Journal of Scientific Computing*, vol.1, no.3, (2003).
- [19] T. Chana, E. Selim, E. Park, "Image decomposition combining staircase reduction and texture extraction", *Journal of Visual Communication and Image Representation*, vol.18, no.6, (2007).
- [20] T. Goldstein, S. Osher, "The Split Bregman Method for L1-Regularized Problems", *SIAM Journal on Imaging Sciences*, vol.2, no.2, (2009).
- [21] Y. Wang, J. Yang, W. Yin, Y. Zhang, "A New Alternating Minimization Algorithm for Total Variation Image Reconstruction", *SIAM Journal on Imaging Sciences*, vol.1, no.3, (2008).
- [22] S. Osher, M. Bureger, D. Goldfarb, J. Xu, W. Yin, "An Iterative Regularization Method for Total Variation-Based Image Restoration", *Multiscale Modeling and Simulation*, vol.4, no.2, (2005).
- [23] X. Bai, F. Zhou, B. Xue, "Image enhancement using multi-scale image features extracted by top-hat transform", *Optics & Laser Technology*, vol. 44, no.2, (2012).
- [24] <http://www.ece.lehigh.edu/spcrl>, online image database, Accessed (2013) April 17.
- [25] <http://www.imagefusion.org/>, Image fusion toolbox, Accessed (2013) March 20.
- [26] <http://www.ifp.illinois.edu/minhdo/software/>, NSCT toolbox, Accessed (2013) January 20.
- [27] [http://tag7.web.rice.edu/Split\\_Bregman\\_files/](http://tag7.web.rice.edu/Split_Bregman_files/), Split Bregman toolbox, Accessed (2013) July 15.
- [28] [http://foulard.ece.cornell.edu/gaubatz/metrix\\_mux/metrix\\_mux\\_1.1.zip](http://foulard.ece.cornell.edu/gaubatz/metrix_mux/metrix_mux_1.1.zip), Assessment Package, Accessed (2013) January 10.
- [29] Z. Wang, A.C. Bovik, H.R. Sheikh, E.P. Simoncelli, "Image quality assessment: from error visibility to structural similarity", *IEEE Transactions on Image Processing*, vol. 13, no. 4, (2004).
- [30] D.J.C. MacKay, "Information theory, inference and learning algorithms", Cambridge university press, (2003).
- [31] C.S. Xydeas, V. Petrovic, "Objective image fusion performance measure", *Electronics Letters*, vol. 36, no. 4, (2000).

## Authors

**Yongxin Zhang** received PhD degree in Computer Software and Theory from Northwest University. He is currently an assistant professor in the School of Information Technology, Luoyang Normal University, Luoyang, China. His research interests include image processing and pattern recognition.

**Hongan Li** received PhD degree in computer software and theory from Northwest University. He is currently an assistant professor in the School of Computer Science and Technology, Xi'an University of Science and Technology, Xi'an, China. His research interests include image processing and pattern recognition.

**Zhihua Zhao** is currently pursuing a PhD degree at the School of Information Science and Technology, Northwest University, Xi'an, China. His research interests include image processing.

